

Original article

Revisiting the role of fluid imbibition in the hydrocarbon recovery processes from shale reservoirs

Boyun Guo^{✉*}, Philip Wortman

College of Engineering, University of Louisiana at Lafayette, Lafayette LA 70504, USA

Keywords:

Shale gas and oil
spontaneous imbibition
capillary pressure
mathematical model
experimental investigation

Cited as:

Guo, B., Wortman, P. Revisiting the role of fluid imbibition in the hydrocarbon recovery processes from shale reservoirs. *Capillarity*, 2025, 15(2): 25-32.
<https://doi.org/10.46690/capi.2025.05.01>

Abstract:

Spontaneous imbibition has recently received a great deal of research attention for improving hydrocarbon recovery from shale gas and oil reservoirs. It is highly desirable to know the true significance and the role of fluid imbibition in the recovery process. Using a Krüss Drop Shape Analyzer 100S with Krüss' Advance software, water imbibition depth was measured in this study on dry cores from four shale gas/oil reservoirs namely Tuscaloosa Marine Shale, Eagle Fort Shale, Marcellus Shale, and Green River Shale. The initial water-contact angles on the Tuscaloosa Marine Shale, Eagle Fort Shale, Marcellus Shale and Green River Shale core surfaces were measured to be 36.62°, 66.68°, 52.78° and 84.73°, respectively. The contact angle and thus volume of liquid droplet changed due to fluid imbibition into the core samples and evaporation. The change in droplet volume, together with the contact area and shale porosity, was used to calculate the imbibition depth. An analytical imbibition model was derived and tuned to upscale the tested fluid imbibition data to field level. The result of time-upscaling using the tuned imbibition models shows that the 1-month water imbibition depths for the Tuscaloosa Marine Shale, Eagle Fort Shale, Marcellus Shale and Green River Shale are 2.61, 1.59, 0.89 and 0.16 cm, respectively. These low values suggest that the direct effect of water imbibition into shale matrix on hydrocarbon recovery in shale reservoirs is insignificant in the practical scales of space and time. However, the imbibition-induced shale cracks can increase shale permeability significantly for mass transfer during the hydrocarbon recovery process. Water imbibition in the cracks should be investigated in future studies.

1. Introduction

Then phenomena of spontaneous imbibition of fluid have attracted a great amount of research in hydrocarbon recovery processes from shale gas and oil and reservoirs. Dutta et al. (2012) presented a quantitative analysis of fracturing fluid imbibition in low-permeability formations. Cai et al. (2014) theoretically investigated spontaneous imbibition in tortuous capillaries of non-circular cross-sections. Zhang et al. (2025) expanded Cai et al. (2014)'s theory to cover capillaries of concave triangle pore channels formed between up to three

different solid materials.

Experimental investigations of spontaneous imbibition in shales have also been investigated. Saidzade et al. (2020) conducted imbibition experiments under one-end-open boundary conditions to simulate the condition in hydraulic-fractured shale gas/oil wells. Fast progress in research and technology development in this area are documented in Li et al. (2019), Shaibu and Guo (2021), and Yang et al. (2023).

Recent studies in the area of spontaneous imbibition focus on upscaling of lab-data to field-level applications. Cai et al. (2023) provides a thorough review of the most recent re-

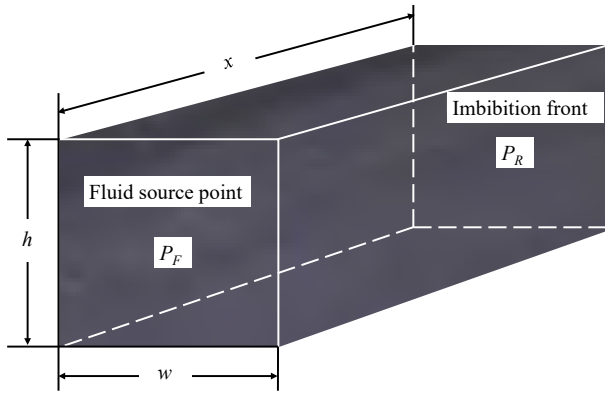


Fig. 1. Sketch to illustrate 1-dimensional fluid imbibition.

search work in this subject. It revealed the complications of the spontaneous imbibition involving multi-influencing factors including multiphase flow and variation in properties of shale and fluids.

Imbibition is mainly driven by capillary pressure induced by Interfacial Tension (IFT). Because capillary pressure increases as pore size decreases, some people believe that the capillary-pressure-induced imbibition is a major cause for hydrocarbon recovery from low-permeability shale gas/oil reservoirs. The fact is that the viscous resistance to fluid imbibition increases as the pore size decreases. The ultimate effect of pore size is that fluid imbibition drops as pore size decreases (Guo and Wortman, 2024; Mahmood et al., 2024). Therefore, it is expected that the effect of fluid spontaneous imbibition on gas/oil recovery is lower in shale gas/oil reservoirs than that in conventional reservoirs. However, this does not rule out spontaneous imbibition as a major factor affecting hydrocarbon recovery in shale gas/oil reservoir because the effect of other factors, such as molecular diffusion and viscous displacement, are also weak in low-permeability porous media.

The best way to evaluate the relative importance of fluid spontaneous imbibition is to run laboratory testing to obtain short-time imbibition data and upscale the test result with a data-tuned mathematical model. One of the challenges in investigation of spontaneous imbibition in shale formations is the measurement of the extremely slow imbibition depth due to the ultra-low permeability of shale. It takes hours and days to detect the measurable changes in fluid volume (Gao et al., 2019; Yang et al., 2023). Evaporation of the fluid to the atmosphere can be so significant to mask the true fluid imbibition effect during the measurement (Yuan et al., 2019). Saidzade et al. (2020) showed that imbibition curve can be interpreted into four regions by the change in the imbibition rate, namely

- 1) fast imbibition region dominated by capillary force,
- 2) transition region,
- 3) slow imbibition region dominated by diffusion force,
- 4) zero-imbibition region due to clay swelling.

Optical goniometry machines use photography to measure the time-dependent height, wetting-diameter, and contact angle of small droplets. After proper image calibration, the time-dependent volume and surface area of the droplet can be calculated. Assuming the volume change of droplet is affected

only by evaporation and imbibition and using the droplet surface area for estimating the volume loss due to evaporation, it is possible to obtain the true volume loss due to sole imbibition.

This study performed short-time optical goniometry measurement and tuned a mathematical model by the measured data to predict the long-term behavior of spontaneous imbibition in shale formation. The result of this investigation indicates that fluid imbibition depth in shale matrix is limited. However, the imbibition-induced cracks in the formation can play a key role in the hydrocarbon recovery processes.

2. Mathematical modeling

Fig. 1 illustrates a piece of shale rock where P_F is fluid pressure at the source point and P_R is pore pressure at the front of fluid imbibition. The fluid mass transfer from the source point into the shale matrix is driven by pressure differential, capillary force, and sometimes molecular diffusion. Fluid flow is resisted by viscous force. For the mass transfer in horizontal orientation, the mass transfer rate is also affected by the pressure differential ($P_F - P_R$) and not affected by gravity. According to Zhang et al. (2021), in porous media of super-low permeabilities, such as cement concrete and shales, the fluid molecular diffusion is an extreme low process. Assuming the effect of molecular diffusion is negligible, a rigorous analytical model for predicting the fluid imbibition in shale rocks was derived in study. If the inertial term is neglected, the following equation should predict the distance, or depth, of imbibition (derivation is available upon request):

$$x = \sqrt{\frac{\sigma \cos \theta + 0.5r_c(P_F - P_R)}{245,250 \frac{\mu_w r_c}{k_{rw} k}}} \quad (1)$$

where x is distance or depth of fluid imbibition (cm), σ is IFT (Dyne/cm), k_{rw} is relative permeability to the imbibing fluid, k is the absolute permeability (Darcy), θ is fluid contact angle, μ_w is fluid viscosity (cp), r_c is the equivalent radius of capillary (cm), and t is time (sec.) This imbibition model is very similar to the one given by Handy (1960)'s except that he assumed that the relative permeability is equal to the saturation of the imbibing fluid and that the effect of pressure differential was neglected.

Eq. (1) describes pressure-assisted imbibition in porous media. If the effect of pressure differential is neglected ($P_F - P_R = 0$), the mass transfer is solely due to spontaneous imbibition expressed by:

$$x = \sqrt{\frac{k_{rw} k \sigma \cos \theta}{245,250 r_c \mu_w}} \quad (2)$$

This equation implies that the balance between the capillary force and resistant force controls the imbibition depth.

3. Measurement of imbibition depth

Shale core surfaces were prepared by polishing the surfaces using an aluminum oxide sandpaper lightly wetted with deionized water stepwise up to 2,000 grit. The surface was cleaned with a small amount of deionized water and a microfiber cloth

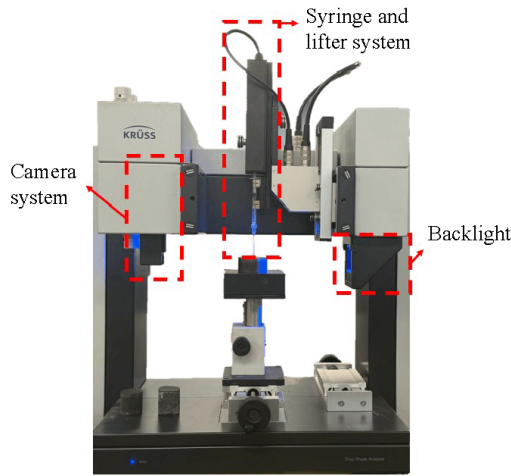


Fig. 2. Krüss drop shape analyzer 100S.

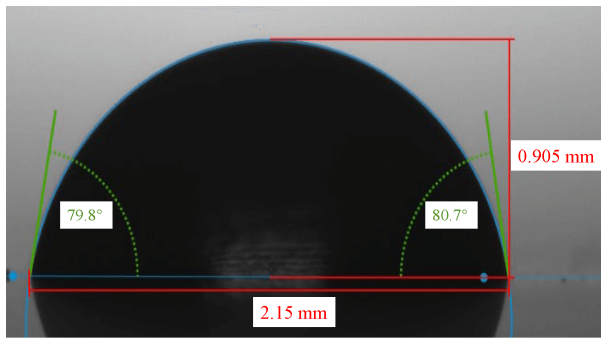


Fig. 3. Enhanced droplet image from a Krüss DSA 100S modified with measured height and width from external software.

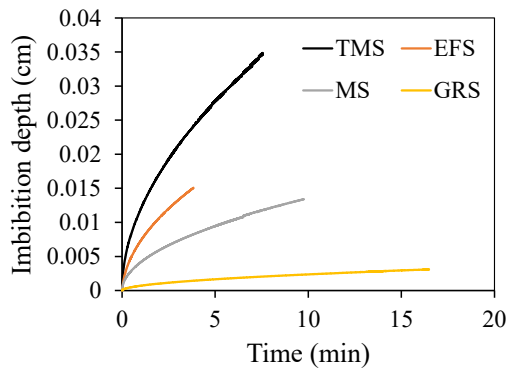


Fig. 4. Calculated water imbibition depth based on measured imbibition volume data for 4 shales.

until no additional abraded material remained on the surface.

Optical goniometer measurements were performed using a Krüss DSA 100S and analyzed with Krüss' Advance software (Fig. 2). Images, such as that shown in Fig. 3, exported from Advance were used to measure the height of the droplet as the software did not perform the measurements internally. Images were exported in 25 second intervals and the heights were interpolated between the measured points. The following procedure was performed to derive the imbibition and evaporation rates:

- 1) Prepare smooth dry surface of shale sample and liquid solution.
- 2) Use an automated syringe system to place a droplet of liquid on the horizontal surface of shale sample, and record droplet volume.
- 3) Measure the initial height, wet diameter, and sessile drop contact angle.
- 4) Calculate the drop volume with a geometric equation (available from the authors upon request) and compare the result with the initial volume of droplet. If they are consistent, the equation is validated.
- 5) Measure and record time-dependent values of height, wet diameter, and contact angle of sessile drop at each timestep.
- 6) Calculate droplet volume and parameter A-value in Hu et al. (2014)'s evaporation equation at each timestep.
- 7) Determine evaporation volume and imbibition volume at each timestep.

Water imbibition was measured on dry cores from four shale gas/oil reservoirs namely Tuscaloosa Marine Shale (TMS), Eagle Fort Shale (EFS), Marcellus Shale (MS), and Green River Shale (GRS). The initial water-contact angles on the TMS, EFS, MS and GRS core surfaces were measured to be 36.62° , 66.68° , 52.78° and 84.73° , respectively.

Fig. 4 presents the water imbibition curves based on measured droplet geometries for the four shales. Porosity data used in the imbibition depth conversion are discussed in the next section.

4. Significance analysis

Significance of water imbibition was investigated for the four reservoirs, i.e., TMS, EFS, GRS, and MS, by predicting the water imbibition depth as a function of imbibition time. The procedure used is as follows:

- Step 1: Estimate the fluid and rock property parameters involved in Eq. (2).
- Step 2: Simulate water imbibition process with Eq. (2).
- Step 3: Tune Eq. (2) with measured imbibition data accounting for uncertainties in parameter values, especially permeability and pore size that are measured for the tested cores. The tuning is performed to minimize the relative error function by changing the value of factor C in the following equation:

$$E_r = \sum_{i=1}^n \frac{(Cx_i)^2 - x_{mi}^2}{x_{mi}^2} \quad (3)$$

where x_i is the imbibition depth calculated by Eq. (2) at time point i , x_{mi} is the measured imbibition depth at time point i , and n is the number of points.

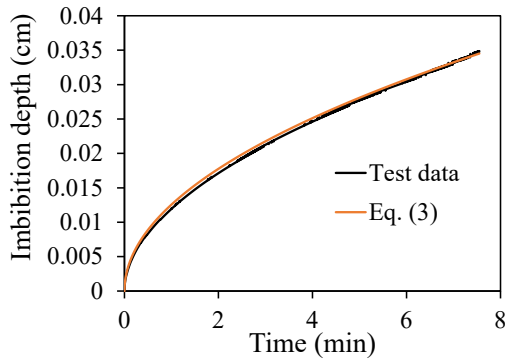
- Step 4: Predict the long-term water imbibition profile with the tuned Eq. (2).
- Step 5: Analyze the long-term significance of the water imbibition.

4.1 Tuscaloosa marine shale

The Tuscaloosa Marine Shale (TMS) was deposited along the northern Gulf of Mexico approximately 95-89 million ye-

Table 1. TMS formation and fluid properties.

| Parameter | Value | Unit |
|---------------------------------|---------|---------|
| Shale porosity | 0.061 | / |
| Equivalent pore diameter | 0.0002 | cm |
| Shale absolute permeability | 0.00021 | md |
| Relative permeability | 0.75 | / |
| Water-shale interfacial tension | 40 | Dyne/cm |
| Water contact angle | 36.62 | deg |
| Water viscosity | 0.8 | cp |

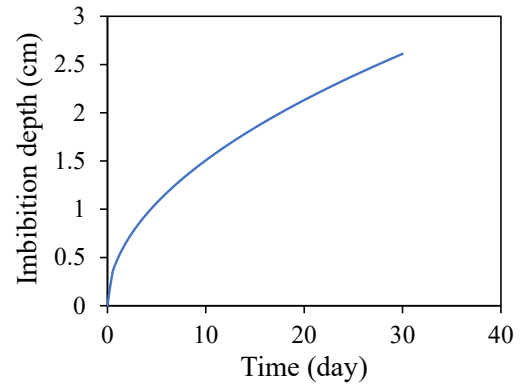
**Fig. 5.** Comparison of water imbibition depths given by test data and Eq. (3) for TMS.

ars ago (Lu et al., 2011). TMS is estimated to contain 1,537 million barrels of oil plus 4,614 billion cubic feet of gas. According to Lu et al. (2015)'s investigation, the porosity TMS is less than 4% and TMS permeability is between 10 and 79 nd. According to the measurement of Lohr and Hackley (2018), the porosity of the TMS is between 3.86% and 9.86% (average 6.1%). The corresponding permeability is between 46 and 2,990 nd (averaged 427 nd). According to Yang and Guo (2020)'s statistical analyses of production data, the effective formation permeability of TMS is 53 to 210 nd. The permeability range was also given by Borrok et al. (2019) and it is close to that given by Yang and Guo (2020). Therefore, the later data set (0.000053 to 0.000210 md with an average 0.000131 md) is used in this study.

Borrok et al. (2019) reported that most samples of TMS are characterized by a total clay content of 40 to 80 wt%, quartz of 20 to 40 wt%, and less than about 40 wt% calcite. TMS exhibits a moderate Total Organic Carbon (TOC) content, averaging around 1.0 wt%, with some samples showing up to 2.8 wt%.

With a fixed value of porosity $\phi = 0.061$, substituting $k = 0.00021$ md into the correlation of Kolodzie Jr. (1980) (modified by Pittman in 1992) and applying Schwartz (1969)'s rule give an estimated average pore sizes of 0.00002 cm. Table 1 presents some data for the TMS.

Fig. 5 shows a comparison of water imbibition depths given by test data and Eq. (2) for TMS with a tuning factor 1.01 to Eq. (2):

**Fig. 6.** Model-predicted water imbibition depth in TMS in the first 30 days.**Table 2.** EFS formation and fluid properties.

| Parameter | Value | Unit |
|---------------------------------|--------|---------|
| Shale porosity | 0.0755 | / |
| Equivalent pore diameter | 0.0006 | cm |
| Shale absolute permeability | 0.0059 | md |
| Relative permeability | 0.65 | / |
| Water-shale interfacial tension | 40 | Dyne/cm |
| Water contact angle | 66.68 | deg |
| Water viscosity | 0.8 | cp |

$$x = 1.01 \sqrt{\frac{k_{rw} k \sigma \cos \theta}{245,250 r_c \mu_w}} t \quad (4)$$

Fig. 6 presents water imbibition depth given by Eq. (3) for TMS for one month of imbibition time. It indicates an imbibition depth of only 2.61 cm, which is considered insignificant for improving hydrocarbon recovery in shale gas/oil reservoirs.

4.2 Eagle ford shale

The Eagle Ford Group in South Texas is a sediment occurrence of about 20 ft thick with a high porosity zone in the Lower Eagle Ford Formation located in central Atascosa County, Texas. It contains a much higher carbonate shale percentage, upwards to 70% in south Texas. The high percentage of carbonate makes it more brittle and therefore more conducive to hydraulic fracturing. Generally, the EFS has a porosity ranging from 5.30% to 9.79% (7.55% average), permeability ranging from 0.006 μ d to 11.8 μ d (5.9 μ d average), and TOC about 6.72%. The density-log porosity was averaged nearly 17% (Finger et al., 2017).

Table 2 presents some data for the EFS where the correlation of Kolodzie Jr. (1980) modified by Pittman (1992) was used to estimate the equivalent pore size.

Fig. 7 shows a comparison of water imbibition depths given by test data and Eq. (2) for EFS with a tuning factor 0.97 to Eq. (2):

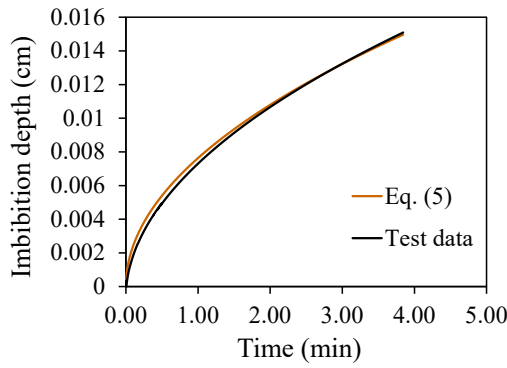


Fig. 7. Comparison of water imbibition depths given by test data and Eq. (5) for EFS.

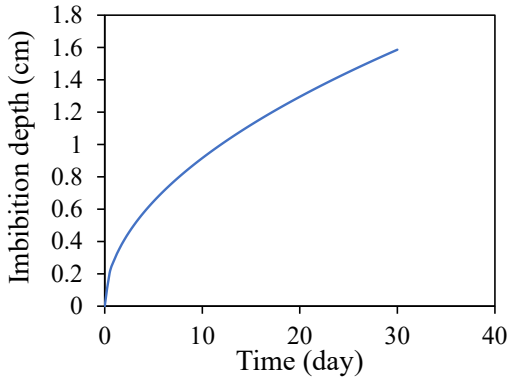


Fig. 8. Model-predicted water imbibition depth in EFS in the first 30 days.

$$x = 0.96 \sqrt{\frac{k_{rw} k \sigma \cos \theta}{245,250 r_c \mu_w} t} \quad (5)$$

Fig. 8 presents water imbibition depth given by Eq. (4) for EFS for one month of imbibition time. It indicates an imbibition depth of only 1.59 cm, which is considered insignificant for improving hydrocarbon recovery in shale gas/oil reservoirs.

4.3 Marcellus shale

MS is a Middle Devonian age unit of sedimentary rock found in eastern North America. Named for a distinctive outcrop near the village of Marcellus, New York, it extends throughout much of the Appalachian Basin. The occurrence of sedimentary structures in the MS such as starved ripples, graded beds, bioturbation, etc., were all interpreted to be indicative of current activity. TOC content was found to increase from the eastern margins of the basin towards the western craton-ward side of the basin. Marcellus black shale facies were thus probably deposited in a bathymetrically subdued setting akin to present-day continental. The Marcellus Shale exhibits relatively high porosity (5-15% in the southwest and 4-10% in the northeast) and surprisingly high permeability (130 to over 2,000 nd, average 1,065 nd), making it a unique and exceptional gas-shale play (Zamirian et al., 2016).

Table 3 presents some data for the MS. The equivalent pore size was estimated by the correlation of Kolodzie Jr. (1980) modified by Pittman (1992).

Table 3. MS formation and fluid properties.

| Parameter | Value | Unit |
|---------------------------------|----------|---------|
| Shale porosity | 0.1 | / |
| Equivalent pore diameter | 0.0005 | cm |
| Shale absolute permeability | 0.001065 | md |
| Relative permeability | 0.65 | / |
| Water-shale interfacial tension | 40 | Dyne/cm |
| Water contact angle | 52.78 | deg |
| Water viscosity | 0.8 | cp |

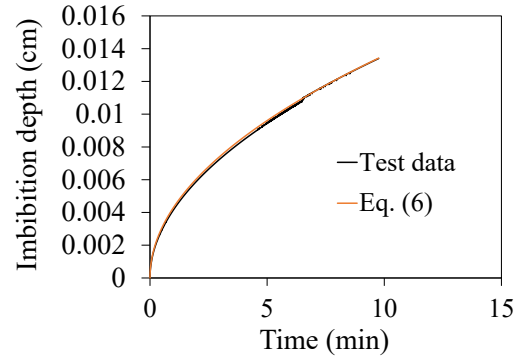


Fig. 9. Comparison of water imbibition depths given by test data and Eq. (6) for MS.

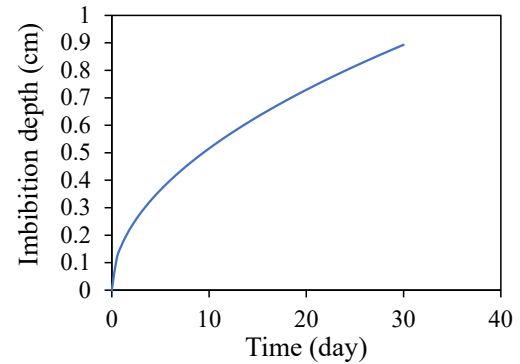


Fig. 10. Model-predicted water imbibition depth in MS in the first 30 days.

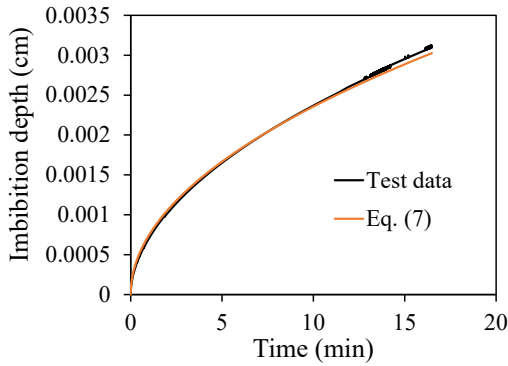
Fig. 9 shows a comparison of water imbibition depths given by test data and Eq. (2) for MS with a tuning factor 0.95 to Eq. (2):

$$x = 0.95 \sqrt{\frac{k_{rw} k \sigma \cos \theta}{245,250 r_c \mu_w} t} \quad (6)$$

Fig. 10 presents water imbibition depth given by Eq. (5) for MS for one month of imbibition time. It indicates an imbibition depth of only 0.89 cm, which is considered insignificant for improving hydrocarbon recovery in shale gas/oil reservoirs.

Table 4. GRS formation and fluid properties.

| Parameter | Value | Unit |
|---------------------------------|---------|---------|
| Shale porosity | 0.1 | / |
| Equivalent pore diameter | 0.001 | cm |
| Shale absolute permeability | 0.00044 | md |
| Relative permeability | 0.65 | / |
| Water-shale interfacial tension | 40 | Dyne/cm |
| Water contact angle | 84.73 | deg |
| Water viscosity | 0.8 | cp |

**Fig. 11.** Comparison of water imbibition depths given by test data and Eq. (7) for GRS.

4.4 Green river shale

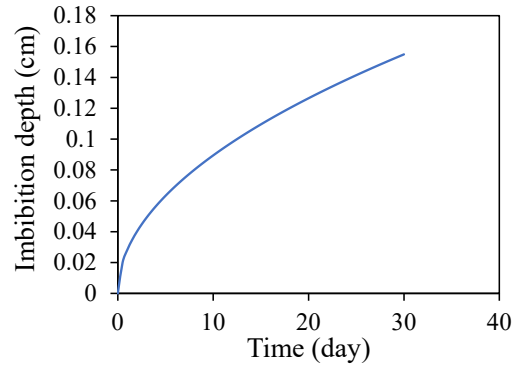
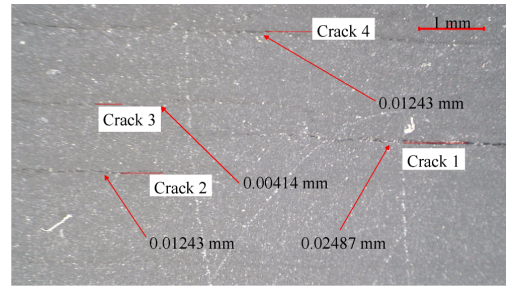
The Green River Shale is part of the Eocene geologic formation presented in Green River in Colorado, Wyoming, and Utah. The lithology of the lake sediments varies including sandstones, mudstones, siltstones, and a variety of lacustrine limestones and dolomites. The porosity of Green River Shale is about 10% for lean oil shale with about 1 wt% TOC. The porosity and permeability of the Green River shale vary with average values in the order of 10% and 0.00044 md, respectively (Burnham, 2017).

Table 4 presents some data for the GRS. The correlation of Kolodzie Jr. (1980) modified by Pittman (1992) was employed to estimate the equivalent pore size.

Fig. 11 shows a comparison of water imbibition depths given by test data and Eq. (2) for GRS with a tuning factor 0.94 to Eq. (2):

$$x = 0.94 \sqrt{\frac{k_{rw} k \sigma \cos \theta}{245,250 r_c \mu_w} t} \quad (7)$$

Fig. 12 presents water imbibition depth given by Eq. (6) for GRS for one month of imbibition time. It indicates an imbibition depth of only 0.16 cm, which is considered insignificant for improving hydrocarbon recovery in shale gas/oil reservoirs.

**Fig. 12.** Model-predicted water imbibition depth in GRS in the first 30 days.**Fig. 13.** Images of an FES core with cracks formed during water imbibition.

5. Discussion

The case studies were carried out using petrophysical data from previous literature, not from self-measurement in this study. This is because measuring petrophysical properties of shale cores in labs, especially permeability, is difficult due to the exceedingly long time of testing. Such details in measurement are beyond the scope of this study. This is why tuning factor is used for validating the imbibition model with measured imbibition data. Given that the results are based on short-term experimental data from small-sized cores and model predictions, it is desirable to study this problem systematically in the future to truly represent actual reservoir conditions.

Although the measured data of water imbibition depth into the shale matrix shows insignificant direct impact on hydrocarbon recovery from shale reservoirs, the matrix imbibition may affect well-performance in different manner, such as creating cracks due to water swelling. Fig. 13 shows images of an FES core with cracks formed during water imbibition. These cracks can increase shale permeability significantly for mass transfer during the hydrocarbon recovery process. Water imbibition in the cracks will be investigated in the next step of study.

It is necessary to compare the importance of the spontaneous imbibition effect to that of the forced imbibition effect by pressure. The difference between these two effects is revealed by the numerator of Eq. (1). The ratio of the forced imbibition effect to the spontaneous imbibition effect is expressed by:

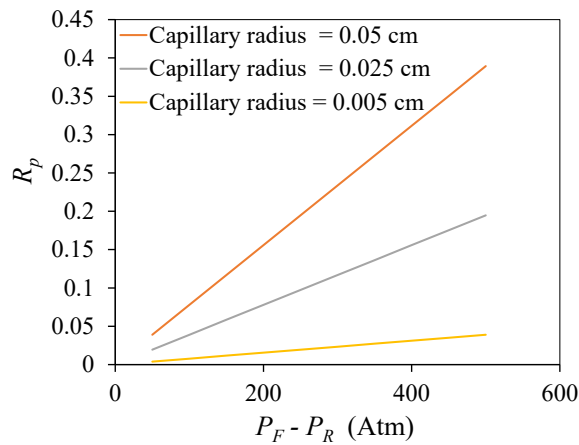


Fig. 14. Factors affecting the ratio of the forced imbibition effect to the spontaneous imbibition effect.

$$R_p = \frac{0.5r_c(P_F - P_R)}{\sigma \cos \theta} \quad (8)$$

This equation is plotted in Fig. 14 for TMS where water-shale interfacial tension is 40 dynes/cm and contact angle is 36.62 degrees. It shows $R_p < 0.4$, meaning that the forced imbibition effect is less than the spontaneous imbibition effect in porous media with pore sizes of less than 0.05 cm.

6. Conclusions

Water imbibition depth was measured on dry cores from four shale gas/oil reservoirs namely TMS, EFS, MS, and GRS, using a Krüss DSA 100S with Krüss' Advance software. An analytical solution was derived to upscale tested fluid imbibition to field level by considering both the spontaneous imbibition driven by capillary pressure and the flow resistance by viscous force. The following conclusions are drawn.

- 1) The initial water-contact angles on the TMS, EFS, MS and GRS core surfaces were measured to be 36.62°, 66.68°, 52.78° and 84.73°, respectively. The contact angle and thus volume of liquid droplet change due to fluid imbibition into the core samples and evaporation. The change in droplet volume, together with the contact area and shale porosity, can be used to calculate the imbibition depth.
- 2) The analytical solution for fluid imbibition can be slightly tuned to match the tested imbibition processes. This tuning procedure is needed to account for the uncertainties in determination of model parameters such as shale permeability and pore size.
- 3) Result of time-upscaling using the tuned imbibition models shows that the 1-month water imbibition depths for the TMS, EFS, MS and GRS are 2.61, 1.59, 0.89 and 0.16 cm, respectively. These low values suggest that the direct impact of water imbibition into shale matrix on hydrocarbon recovery in shale gas/oil reservoirs is insignificant in the practical scales of space and time. However, the imbibition-induced shale cracks can increase shale permeability significantly for mass transfer during the hydrocarbon recovery process. Water imbibition in the cracks should be investigated in future studies.

Acknowledgements

The authors thank the Energy Institute of Louisiana (EIL) at the University of Louisiana at Lafayette for its support to this research.

Conflict of interest

The authors declare no competing interest.

Open Access This article is distributed under the terms and conditions of the Creative Commons Attribution (CC BY-NC-ND) license, which permits unrestricted use, distribution, and reproduction in any medium, provided the original work is properly cited.

References

- Berg, R. R. Method of determining permeability from reservoir rock properties. *Transactions of Gulf Coast Association of Geological Societies*, 1970, 20: 303-317.
- Borrok, D. M., Yang, W., Wei, M., et al., Heterogeneity of the mineralogy and organic content of the Tuscaloosa Marine Shale. *Marine and Petroleum Geology*, 2019, 109, 717-731.
- Burnham, A. K. Porosity and permeability of Green River oil shale and their changes during retorting, *Fuel*, 2017, 203: 208-213.
- Cai, J., Perfect, E., Cheng, C., et al. Generalized modeling of spontaneous imbibition based on Hagen-Poiseuille flow in tortuous capillaries with variably shaped apertures. *Langmuir*, 2014, 30(18): 5142-5151.
- Cai, J., Sun, S., Wang, H. Current advances in capillarity: Theories and applications. *Capillarity*, 2023, 7(2): 25-31.
- Dutta, R., Lee, C., Odumabo, S., et al. Quantification of fracturing fluid migration due to spontaneous imbibition in fractured tight formations. Paper SPE 154939 Presented at the SPE Americas Unconventional Resources Conference, Pittsburgh, Pennsylvania, 5-7 June, 2012.
- Finger, L. J., Godet, A., Billingsley, L. T. Porosity evaluation in the Lower Eagle Ford Shale Formation, Atascosa County, South Texas. *Gulf Coast Association of Geological Societies Transactions*, 2017, 67: 587.
- Gao, Z., Fan, Y., Hu, Q., et al. A review of shale wettability characterization using spontaneous imbibition experiments. *Marine and Petroleum Geology*, 2019, 109: 330-338.
- Guo, B., Wortman, P. Understanding the post-frac soaking process in multi-fractured shale gas-oil wells. *Capillarity*, 2024, 12(1): 6-16.
- Handy, L. L. Determination of effective capillary pressures for porous media from imbibition data. *Transactions of the AIME*, 1960, 219(1): 75-80.
- Hu, D., Wu, H., Liu, Z. Effect of liquid-vapor interface area on the evaporation rate of small sessile droplets. *International Journal of Thermal Sciences*, 2014, 84: 300-308.
- Johnson, R. C., Mercier, T. J., Brownfield, M. E., et al. Assessment of in-place oil shale resources of the Green River Formation, Greater Green River Basin in Wyoming, Colorado, and Utah. USA, U.S. Geological Survey, 2011.
- Kolodzie Jr., S. Analysis of pore throat size and use of the

- Waxman-Smits equation to determine OOIP in spindle field, Colorado. Paper SPE 9382 Presented at the SPE Annual Technical Conference and Exhibition, Dallas, 21-24 September 1980.
- Li, C., Singh, H., Cai, J. Spontaneous imbibition in shale: A review of recent advances. *Capillarity*, 2019, 2(2): 17-32.
- Lohr, C. D., Hackley, P. C. Using mercury injection pressure analyses to estimate sealing capacity of the Tuscaloosa marine shale in Mississippi, USA: Implications for carbon dioxide sequestration. *International Journal of Greenhouse Gas Control*, 2018, 78: 375-387.
- Lu, J., Milliken, K., Reed, R. M., et al. Diagenesis and sealing capacity of the middle Tuscaloosa mudstone at the Cranfield carbon dioxide injection site, Mississippi, USA. *Environmental Geosciences*, 2011 18(1): 35-53.
- Lu, J., Ruppel, S. C., Rowe, H. D. Organic matter pores and oil generation in the Tuscaloosa marine shale. *AAPG Bulletin*, 2015, 99(2): 333-357.
- Mahmood, M. H., Nguyen, V., Guo, B. Challenges in mathematical modeling of dynamic mass transfer controlled by capillary and viscous forces in spontaneous fluid imbibition processes. *Capillarity*, 2024, 11(2): 53-62.
- Pittman, E. D. Relationship of porosity and permeability to various parameters derived from mercury injection-capillary pressure curves for sandstone. *American Association of Petroleum Geologists Bull*, 1992, 76(2): 191-198.
- Saidzade, A., Liu, N., Mokhtari, M., et al. Spontaneous imbibition in shales under one-end-open boundary condition: Effect of wettability, porosity, and bedding orientation. Paper Presented at Unconventional Resources Technology Conference, Virtual, 20-22 July, 2020.
- Schwartz, D. H. Successful sand control design for high rate oil and water wells. *Journal of Petroleum Technology*, 1969, 21(9): 1193-1198.
- Shaibu, R., Guo, B. The dilemma of soaking a hydraulically fractured horizontal shale well prior to flowback-A decade literature review. *Journal of Natural Gas Science and Engineering*, 2021, 94: 104084.
- Yang, X., Guo, B. Statistical analyses of reservoir and fracturing parameters for a multifractured shale oil reservoir in Mississippi. *Energy Science & Engineering*, 2020, 8(3): 616-626.
- Yang, Y., Wang, S., Feng, Q., et al. Imbibition mechanisms of fracturing fluid in shale oil formation: A review from the multiscale perspective. *Energy & Fuels*, 2023, 37(14): 9822-9840.
- Yuan, X., Yao, Y., Liu, D., et al. Spontaneous imbibition in coal: Experimental and model analysis. *Journal of Natural Gas Science and Engineering*, 2019, 67: 108-121.
- Zamirian, M., Aminian, K., Ameri, S. Measuring Marcellus shale petrophysical properties. Paper SPE 180366 Presented at the SPE Western Regional Meeting, Anchorage, Alaska, USA, 23-26 May, 2016.
- Zhang, J., Guo, B., Amponsah, V. N. B. A more rigorous mathematical model for capillary imbibition of CO₂ in shale gas formations. *Capillarity*, 2025, 14(3): 63-71.
- Zhang, P., Guo, B., Liu, N. Numerical simulation of CO₂ migration into cement sheath of oil/gas wells. *Journal of Natural Gas Science and Engineering*, 2021, 94: 104085.